

Polyakov loop fluctuations and deconfinement in the limit of heavy quarks

Pok Man Lo,¹ Bengt Friman,¹ and Krzysztof Redlich^{2,3}

¹*GSI, Helmholtzzentrum für Schwerionenforschung, Planckstr. 1, D-64291 Darmstadt, Germany*

²*Institute of Theoretical Physics, University of Wrocław, PL-50204 Wrocław, Poland*

³*Extreme Matter Institute EMMI, GSI, Planckstr. 1, D-64291 Darmstadt, Germany*

(Dated: July 17, 2018)

We explore the influence of heavy quarks on the deconfinement phase transition in an effective model for gluons interacting with dynamical quarks in color SU(3). With decreasing quark mass, the strength of the explicit breaking of the Z(3) symmetry grows and the first-order transition ends in a critical endpoint. The nature of the critical endpoint is examined by studying the longitudinal and transverse fluctuations of the Polyakov loop, quantified by the corresponding susceptibilities. The longitudinal susceptibility is enhanced in the critical region, while the transverse susceptibility shows a monotonic behavior across the transition point. We investigate the dependence of the critical endpoint on the number of quark flavors at vanishing and finite quark density. Finally we confront the model results with lattice calculations and discuss a possible link between the hopping parameter and the quark mass.

PACS numbers: 12.38.Mh, 11.10.Wx, 25.75.Nq, 11.15.Ha, 24.60.-k, 05.70.Jk

I. INTRODUCTION

In the limit of infinitely heavy quarks, deconfinement in the SU(3) gauge theory is associated with the spontaneous breaking of the Z(3) center symmetry [1–5]. The phase transition is of first-order and is therefore stable against small explicit symmetry breaking [6]. The presence of dynamical quarks breaks the center symmetry explicitly, with a strength that increases as the quark mass decreases. It is thus expected that the transition remains discrete in the heavy quark region, and becomes continuous at some critical value of quark mass [7]. This defines the critical endpoint (CEP) for the deconfinement phase transition.

The relevant observables to study deconfinement are the Polyakov loop and its susceptibilities. Recently these quantities were computed on the lattice within SU(3) pure gauge theory [8]. In particular, the ratio of the transverse and longitudinal Polyakov loop susceptibility was shown to exhibit a θ -like behavior at the critical temperature T_d , with almost no dependence on temperature on either side of the transition. This feature makes such ratios ideal probes of deconfinement.

The influence of the dynamical light quarks on these susceptibilities has been studied in 2- and (2+1)-flavor QCD [9, 10]. The resulting susceptibility ratios are considerably smoothened, reflecting the crossover nature of the transition. However, the theoretical understanding of these observables is still incomplete. It is therefore useful to explore the properties of the Polyakov loop susceptibilities for different number of flavors, as functions of the quark mass in the heavy quark region, thus bridging the gap between pure gauge theory and QCD.

The thermodynamics of SU(3) gauge theory with heavy quarks have long been studied in an effective theory [7] and on the lattice [11–19]. The nature of the deconfinement CEP was recently examined within the effective matrix model [20]. One key finding of this study is that the model results for the critical point depend strongly on the structure of the phenomenological gluon potential.

In this work we reexamine the phase structure of the decon-

finement transition for heavy quarks. We formulate an effective theory where the gluon potential is constructed using the pure lattice gauge theory results on the equation of state and on fluctuations of the Polyakov loop [10]. The contribution from heavy quarks is described by the one loop thermodynamic potential of fermions coupled to a background gluon field [21].

To study the deconfinement CEP, it is essential that the phenomenological gluon potential reproduces not only the equation of state and the Polyakov loop, but also the pure gauge theory results for fluctuations of the Polyakov loop. Thus, we employ the effective Polyakov loop potential of Ref. [10], where both the location of minimum and the curvature are constrained by lattice results. This distinguishes this work from previous studies [20].

We focus on the behavior of the Polyakov loop susceptibilities near the CEP at vanishing and finite quark chemical potential. We also investigate the quark mass dependence of the critical temperature of the CEP for different number of flavors. We find that the longitudinal Polyakov loop susceptibility is strongly enhanced in the critical region, and hence, can be used to probe the location of the CEP. On the other hand, the transverse fluctuations are insensitive to the continuous phase transition, showing monotonic behavior across the critical endpoint.

For a comparison of model and lattice results, we utilize the hopping parameter expansion of the fermionic determinant. Moreover, we propose a tentative relation between the hopping parameter and the quark mass in the continuum limit.

The paper is organized as follows. In the next section, we introduce the effective model for deconfinement in the presence of heavy quarks. We calculate the properties of different susceptibilities and locate the deconfinement critical endpoint. In Sec. III we relate the effective model result and lattice data. In Sec. IV we present our conclusions.

II. MODELING DECONFINEMENT IN THE PRESENCE OF QUARKS

To explore the influence of heavy quarks on the deconfinement phase transition in the SU(3) gauge theory, we consider the following model for the partition function [7, 21–24],

$$Z = \int dL d\bar{L} \det[\hat{Q}_F] e^{-\beta V \hat{U}_G(L, \bar{L})}, \quad (1)$$

where $\beta = T^{-1}$ is the inverse temperature, L is the Polyakov loop and \bar{L} its conjugate. Furthermore, \hat{U}_G is the Z(3) invariant Polyakov loop potential extracted from pure gauge theory, including the contribution of the SU(3) Haar measure. The quark contribution is represented by the determinant of the fermionic matrix \hat{Q}_F , which in the uniform background gluon field A_4 , reads

$$\hat{Q}_F = (-\partial_\tau + \mu - igA_4)\gamma^0 + i\vec{\gamma} \cdot \nabla - m. \quad (2)$$

For N_f degenerate flavors of quark mass m , we obtain the one loop expression [21],

$$\ln \det[\hat{Q}_F] = 2V\beta N_f \int \frac{d^3k}{(2\pi)^3} (3E(k) + g^+ + g^-), \quad (3)$$

where the first term is the vacuum contribution, with $E(k) = \sqrt{k^2 + m^2}$, and

$$g^+ = T \ln(1 + 3Le^{-\beta E^+} + 3\bar{L}e^{-2\beta E^+} + e^{-3\beta E^+}) \quad (4)$$

is the contribution of quarks coupled to the Polyakov loop, with $E^+ = E(k) - \mu$. The function g^- describes the anti-quarks, and is obtained from Eq.(4) by replacing $\mu \rightarrow -\mu$ and $L \leftrightarrow \bar{L}$.

The thermodynamic potential density $\Omega = -(T/V) \ln Z$ is obtained from Eq.(1) in the mean field approximation,

$$T^{-4}\Omega = U_G(L, \bar{L}) + U_Q(L, \bar{L}), \quad (5)$$

where U_Q is the fermion contribution to the effective potential and the thermal averaged Polyakov loop, L and \bar{L} , satisfy the gap equations,

$$\partial\Omega/\partial L = 0, \quad \partial\Omega/\partial \bar{L} = 0. \quad (6)$$

For the pure gluon part U_G , we employ the following phenomenological Polyakov loop potential [10],

$$U_G = -\frac{1}{2}A(T)\bar{L}L + B(T)\ln M_H + \frac{1}{2}C(T)(L^3 + \bar{L}^3) + D(T)(\bar{L}L)^2, \quad (7)$$

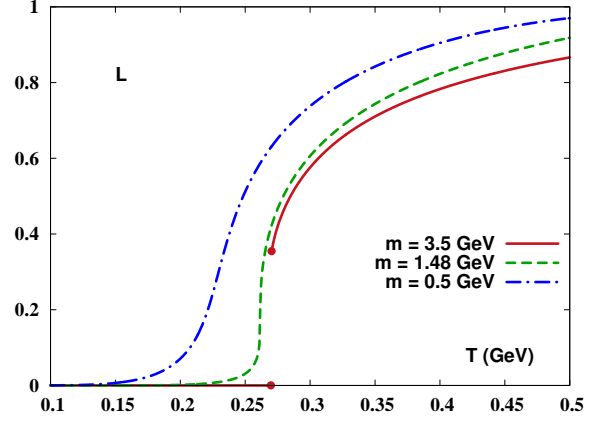


FIG. 1: Temperature dependence of the thermal averaged Polyakov loop for quark masses $m = 0.5, 1.48$ and 3.5 GeV at $N_f = 3$.

where the SU(3) Haar measure M_H , is given by

$$M_H = 1 - 6\bar{L}L + 4(L^3 + \bar{L}^3) - 3(\bar{L}L)^2. \quad (8)$$

The potential (7) was constructed so as to describe the lattice data on SU(3) thermodynamics, including fluctuations of the Polyakov loop. The gluonic potential U_G yields a first-order deconfinement phase transition at the critical temperature, $T_d = 0.27$ GeV.

The quark contribution to the mean field potential is obtained from (3),

$$U_Q = -2N_f\beta^4 \int \frac{d^3k}{(2\pi)^3} [g^+ + g^-], \quad (9)$$

where the vacuum term has been dropped, since it is a constant, independent of the Polyakov loop.

The thermodynamic potential in (5) is the effective model for exploring the thermodynamics of gluons in the presence of heavy quarks.

A. Heavy quarks and deconfinement

The first-order nature of the deconfinement phase transition in the SU(3) pure gauge theory is directly related to the global Z(3) center symmetry and its spontaneous breaking. This transition is eventually washed out by the explicit symmetry breaking induced by the finite quark mass. These features are clearly exhibited in the mean field model. Indeed, in the limit of large quark masses, the leading order term in U_Q in Eq.(3) is linear in the Polyakov loop. One finds, for $\mu = 0$,

$$U_Q(L, \bar{L}) \approx -h(m, N_f, T) L_L, \quad (10)$$

where L_L is the thermal average of the longitudinal Polyakov

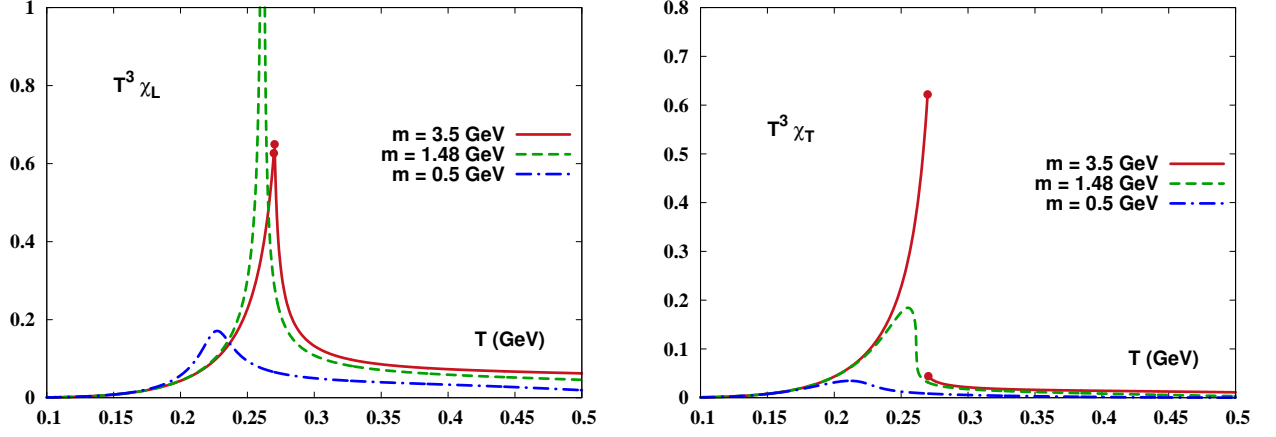


FIG. 2: The temperature dependence of the longitudinal χ_L and the transverse χ_T Polyakov loop susceptibility for $N_f = 3$ and quark masses, $m = 0.5, 1.48, 3.5$ GeV.

loop¹, and

$$h(\beta m, N_f) = \frac{6N_f}{\pi^2 T^3} \int dk k^2 e^{-\beta E}, \quad (11)$$

is a dimensionless function of N_f and βm .

Equation (10) clearly shows that finite mass quarks generate an external field for the Polyakov loop that breaks the $Z(3)$ symmetry explicitly. Clearly, in the limit $\beta m \rightarrow \infty$, the strength of this field vanishes and the thermodynamics of pure gauge theory is recovered.

The strength of the symmetry breaking term increases with decreasing quark mass, eventually turning the first-order deconfinement transition into a crossover. Consequently, there is a critical value of the quark mass, m_{CEP} , where the first-order transition ends at a second order critical endpoint [7].

Using the linear symmetry breaking term (10), the location of the second order CEP is determined by [20]

$$h((\beta m)_{\text{CEP}}, N_f) = h_c, \quad (12)$$

where h_c is a dimensionless constant, to be determined. The value of h_c depends only on the Polyakov loop potential U_G . Since $h(\beta m)$ in (10) is a decreasing function of βm , Eqs.(11) and (12) imply that the ratio $m_{\text{CEP}}/T_{\text{CEP}}$ increases with N_f . Naturally, such a pattern is also observed when the full one loop quark potential (9) is employed.

Details of the phase structure of the deconfinement transition are revealed by examining the Polyakov loop fluctuations. In the following, we study how the position of the CEP changes with the number of quark flavors at vanishing and at finite quark density.

B. The deconfinement critical endpoint at $\mu = 0$

At $\mu = 0$, the thermal average of the transverse Polyakov loop L_T vanishes, due to the symmetry of the partition function (1). Consequently, only the longitudinal Polyakov loop L_L serves as an order parameter for deconfinement. On the other hand, both the longitudinal and transverse fluctuations of the Polyakov loop are non-vanishing. We introduce the longitudinal χ_L and transverse χ_T susceptibilities

$$\chi_{L,T} = \frac{1}{2} V (\langle L\bar{L} \rangle_c \pm \langle LL \rangle_c), \quad (13)$$

where $\langle \dots \rangle_c$ denotes the connected part. The two terms on the r.h.s of Eq.(13) are obtained by taking the appropriate field derivatives [10, 25] of the thermodynamic potential (5).

The influence of heavy quarks on the deconfinement transition is clearly reflected by the properties of the Polyakov loop. In Fig. 1 we show the Polyakov loop as a function of temperature for three values of the quark mass. The expectation value of the Polyakov loop, $\langle L \rangle$ is determined by the position of the global minimum of the potential (5), including the complete one loop quark contribution (9) for three degenerate quark flavors.

For a sufficiently large quark mass, the first-order nature of the phase transition persists, while at smaller quark masses, the explicit symmetry breaking is stronger and the transition is of the crossover type. The endpoint of the line of first-order transitions defines the critical value of the quark mass, m_{CEP} .

To identify the CEP, we consider the longitudinal fluctuations of the Polyakov loop. At the CEP, the longitudinal susceptibility χ_L diverges whereas the transverse susceptibility χ_T remains finite.

In Fig. 2 we show the longitudinal and transverse susceptibility for three degenerate quark flavors. While both susceptibilities depend on the value of the quark mass, only the longitudinal one shows enhancement near the CEP. The transverse susceptibility decreases monotonically with decreasing

¹ In the real sector of the $Z(3)$ target space, the longitudinal L_L and transverse L_T parts of the Polyakov loop correspond to the real and imaginary parts respectively.

quark mass. Thus, for a given N_f , the CEP can be located by identifying the global maximum of χ_L . Our results for the critical quark masses obtained for different number of quark flavors at the CEP are as follows,

$$m_{\text{CEP}} = 1.10, 1.35, 1.48 \text{ GeV, for } N_f = 1, 2, 3. \quad (14)$$

The resulting trend, with m_{CEP} increasing with N_f , is consistent with previous findings [20]. However, we obtain a lower value of the critical quark mass than that found in the matrix model, $m_{\text{CEP}} \simeq 2.5 \text{ GeV}$ at $N_f = 3$. As discussed in Ref. [20], the location of the deconfinement critical endpoint is very sensitive to the form of the Polyakov loop potential. In the present calculation, U_G reproduces the lattice data on the equation of state as well as on the susceptibilities of the Polyakov loop. This feature is crucial for locating the CEP, which is influenced by fluctuations of the order parameter.

At a given value of the quark mass, we identify the deconfinement transition with the location of the maximum of χ_L . In Fig. 3 we show the resulting phase diagram in the (T, m) -plane for different N_f . We observe that the temperature of the CEP remains almost constant at $T_{\text{CEP}} \simeq 0.261 \text{ GeV}$ for all N_f . This value is lower than the critical temperature in the pure gauge theory by about 9 MeV. Here, the temperature obtained in the matrix model is essentially zero [20].

The very weak dependence of T_{CEP} on N_f , seen in Fig. 3, can be qualitatively understood. Assuming the structure of the thermodynamic potential introduced in Eq.(5), and keeping only the leading symmetry breaking term, $U_Q \approx -hL_L$, the conditions for the CEP are

$$\frac{\partial U_G}{\partial L_L} = h, \quad \frac{\partial^2 U_G}{\partial L_L^2} = 0, \quad \text{and} \quad \frac{\partial^3 U_G}{\partial L_L^3} = 0. \quad (15)$$

The first condition in Eq.(15) is just the gap equation, while the second and the third conditions reflect the fact that at the CEP, three extrema of the effective potential merge. The solution of Eq.(15) fixes the critical values of the Polyakov loop, the quark mass and the temperature, L_{CEP} , m_{CEP} , and T_{CEP} . If U_G is independent of the quark mass, the last two conditions in (15) uniquely determine T_{CEP} and L_{CEP} . Thus, in the heavy quark limit, where the leading symmetry breaking term (10) dominates, the critical temperature of the CEP, T_{CEP} , is independent of N_f .

A dependence of the effective Polyakov loop potential on the quark mass m naturally appears when the complete one loop quark contribution in Eq.(3) is used. The fact, that T_{CEP} is almost N_f independent, as shown in Fig. 3, confirms the expectation that the leading term in U_Q , shown in Eq.(10), is sufficient in the mass range considered.

C. Phase diagram at finite chemical potential

At finite μ , the expectation values of the Polyakov loop L , and its conjugate \bar{L} are both real, but in general, different [25–27]. This is because at non-zero μ the effective action is complex [25, 27].

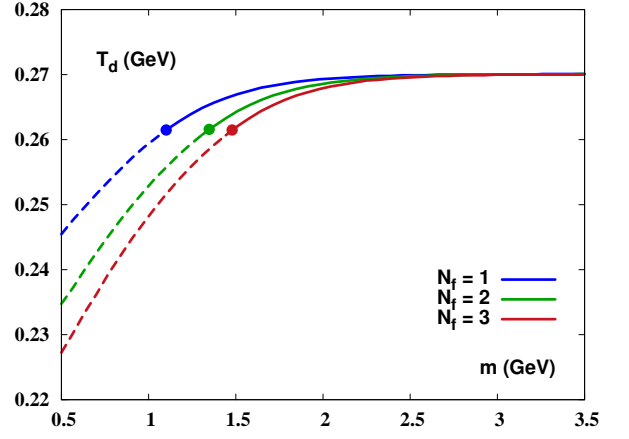


FIG. 3: Quark mass dependence of the deconfinement temperature, defined by a peak of χ_L , for different N_f . Full lines correspond to the first-order phase transitions, while dashed lines represent the pseudo-critical temperature of the crossover transition. The points indicate the locations of the CEP.

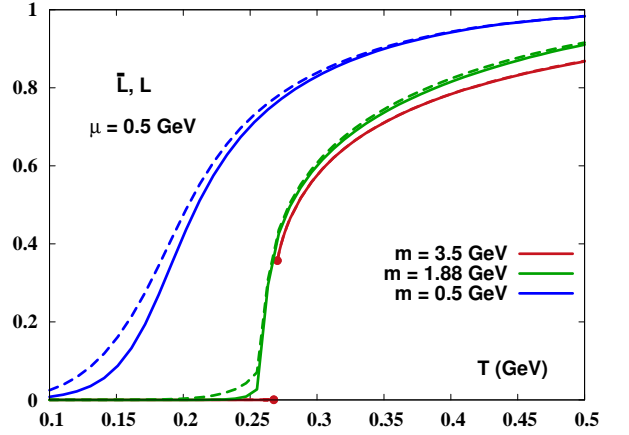


FIG. 4: The expectation values of the Polyakov loop L (full lines) and its conjugate \bar{L} (dashed lines) at $\mu = 0.5 \text{ GeV}$, and for different values of the quark mass, $m = 3.5, 1.88, 0.5 \text{ GeV}$. (from right to left)

The expectation values of L and \bar{L} are determined by solving the gap equations:

$$\frac{\partial \Omega}{\partial L} = 0, \quad \text{and} \quad \frac{\partial \Omega}{\partial \bar{L}} = 0, \quad (16)$$

with the thermodynamic potential Ω given in Eq.(5).

In Fig. 4 we show the temperature dependence of L and \bar{L} for finite μ , and for several values of the quark mass with $N_f = 3$. While \bar{L} and L differ below the deconfinement transition, they merge at high temperatures. This follows from the restriction of (L_L, L_T) target region, imposed by the Haar measure. In the deconfined phase, as $L_L \rightarrow 1$, the target region enforces $L_T \rightarrow 0$, and thus the difference between \bar{L} and L vanishes. Such a feature is absent in the polynomial type

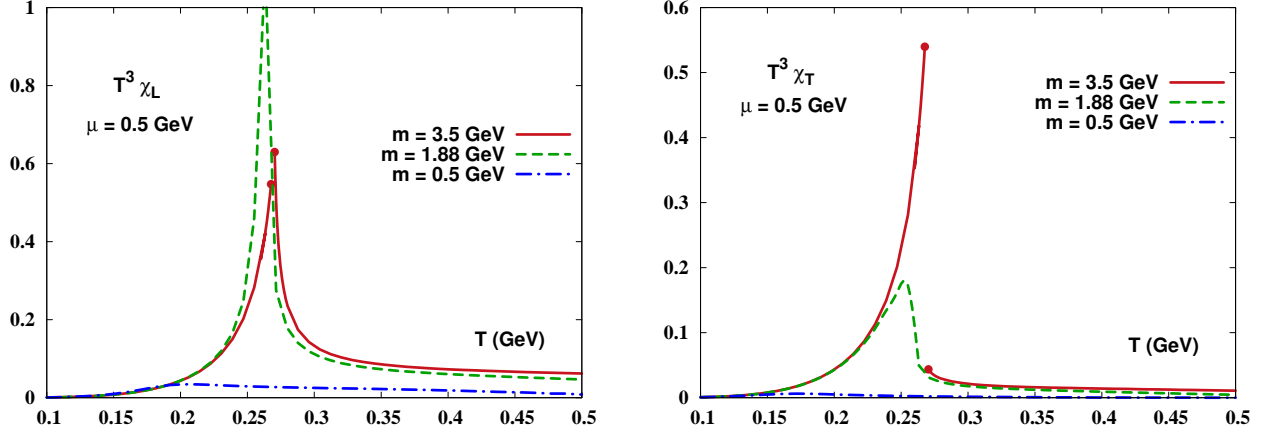


FIG. 5: The longitudinal χ_L and transverse χ_T susceptibility (17), versus T at $\mu = 0.5$ GeV, and for different quark mass values.

potential, which does not comply with the constraints of the SU(3) color group structure [25].

The location of the CEP at finite density is again indicated by a divergence of the longitudinal susceptibility. However, at finite μ , the definitions of the longitudinal and transverse susceptibilities are modified [25]

$$\chi_{L,T} = \frac{1}{2} V [\langle L\bar{L} \rangle_c \pm \frac{1}{2} \langle (LL + \bar{L}\bar{L}) \rangle_c]. \quad (17)$$

For $\mu \rightarrow 0$, $\langle \bar{L}\bar{L} \rangle \rightarrow \langle LL \rangle$, and the above definitions connect smoothly to that, introduced in Eq.(13) for vanishing density.

The finite density results for the longitudinal and transverse susceptibilities are shown in Fig. 5. As for $\mu = 0$, only the longitudinal susceptibility is enhanced near the CEP, whereas the transverse susceptibility is insensitive to criticality.

To construct the phase diagram, we trace the peak location of χ_L as a function of T , μ and m . In Fig. 6 we show the transition temperature as a function of μ at fixed quark mass $m = 1.6$ GeV. This value is larger than the critical mass found at $\mu = 0$, $m_{\text{CEP}} \simeq 1.48$ GeV. Hence, in this case, the transition is first-order at small μ .

As the quark chemical potential increases, the strength of the explicit breaking of the Z(3) symmetry increases and the transition turns into a crossover. These two regimes are connected by the deconfinement CEP, located at the critical chemical potential μ_{CEP} . Clearly, for $m < 1.48$ GeV, the system is in the crossover regime for any value of μ .

The critical temperature $T_{\text{CEP}} \simeq 0.261$ GeV, remains close to its $\mu = 0$ value. This follows from the assumption that U_G is not renormalized by quark loops, which, as discussed above, is reasonably well justified in the parameter range of interest. As m increases, the CEP moves to larger μ , while the critical temperature remains almost constant.

In Fig. 7 we show the dependence of the critical quark mass m_{CEP} on the chemical potential μ . The data points in the figure are extracted from the divergence of χ_L , while the line is determined using the leading term in the heavy quark limit, as discussed below. The increase of the critical quark mass with

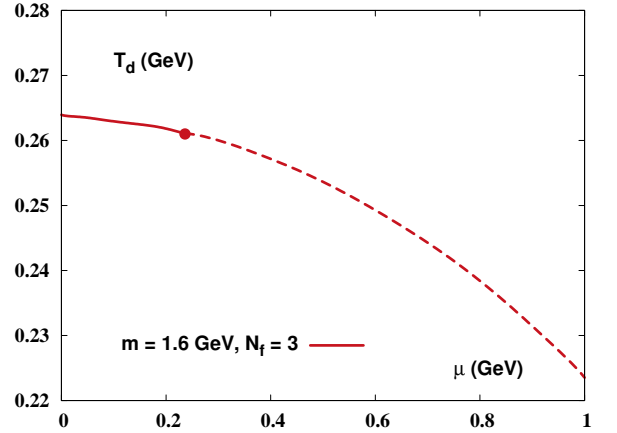


FIG. 6: The μ dependence of the deconfinement temperature, defined by the peak of χ_L , for $m = 1.6$ GeV and $N_f = 3$. The full line corresponds to a first-order phase transition, while the dashed line represents the pseudo-critical temperature of the crossover transition. The point indicates the location of the CEP.

μ , indicates that the first-order region shrinks with increasing density. This finding is consistent with the lattice results presented in Ref. [14, 15].

The relation between m_{CEP} and μ_{CEP} , shown in Fig. 7, can also be studied using the leading contribution to U_Q . At finite μ , one finds

$$U_Q \simeq -h(\beta\mu, \beta m, N_f) L_L, \quad (18)$$

where $L_L = (L + \bar{L})/2$ is the longitudinal Polyakov loop ².

² We have neglected a subleading term in U_Q , which is linear in the transverse Polyakov loop, $L_T = (\bar{L} - L)/2$, since $L_T/L_L \ll 1$ for $T > 0.2$ GeV. (see Fig. 4)

For $m/T \gg 1$, the strength of the symmetry breaking parameter is then given by

$$h(\beta m, \beta \mu, N_f) \simeq \frac{6N_f}{\pi^2} (\beta m)^2 K_2(\beta m) \cosh(\beta \mu), \quad (19)$$

where K_n is the modified Bessel function of the second kind. As discussed above, the phase boundary is determined by

$$h(\beta m, \beta \mu, N_f) = h_c. \quad (20)$$

Since h_c is a universal constant, depending only on the effective Polyakov loop potential, it can be determined at $\mu = 0$. Plugging in the critical quark mass $m_{\text{CEP}} = 1.48$ GeV, the critical temperature $T_{\text{CEP}} = 0.261$ GeV for $N_f = 3$ and $\mu = 0$, one finds, $h_c \approx 0.17$.

In the parameter range considered, the critical temperature at the deconfinement CEP is both μ and N_f independent, and coincides with T_{CEP} at $\mu = 0$. Thus, Eq.(20) defines the relation between the critical quark mass and chemical potential at the CEP

$$\mu_{\text{CEP}} = T_{\text{CEP}} \cosh^{-1} \left(h_c / \left(\frac{6N_f}{\pi^2} ((\beta m_{\text{CEP}})^2 K_2(\beta m_{\text{CEP}})) \right) \right). \quad (21)$$

The solution of the above equation for $N_f = 3$ is shown in Fig. 7. One finds a very satisfactory agreement between $m_{\text{CEP}}(\mu)$ obtained from the global maximum of χ_L and the approximate result from Eq.(21). This indicates, that to quantify the heavy-quark phase diagram at finite density, it is sufficient to retain the leading term (18) in the fermion thermodynamic potential.

III. MODEL PREDICTIONS AND LATTICE RESULTS

In constructing the effective model we assume that the parameters in the gluonic potential U_G are unaffected by the presence of heavy quarks, and that the coupling of quarks to the Polyakov loop is described by the one loop potential. It is important to note, however, that polarization corrections to the transverse gluons is a potential source of m dependence of the parameters of U_G . This is because, in the Polyakov loop potential the transverse gluons are integrated out. If this effect can be neglected, the CEP transition temperature will remain approximately N_f and μ independent. However, one expects that the dressing with fermion loops is important for light quarks. It is therefore interesting to validate these assumptions with first principle calculations on the lattice [16, 19].

Various lattice studies are available for the deconfinement phase transition of heavy flavors [11, 14, 16, 19]. However, the extrapolation to the continuum has not yet been done, and hence, a direct comparison to effective model is uncertain. Nevertheless, some valuable conclusions can be drawn from a comparison of the two approaches.

On the lattice, the fermionic determinant is usually expanded in terms of the lattice hopping parameter κ . The leading term in this expansion reads [19]

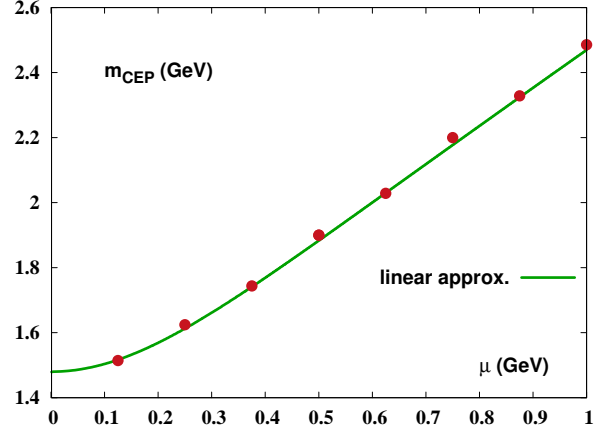


FIG. 7: The critical quark mass as a function of the quark chemical potential for $N_f = 3$. Solid points represent results obtained from the global maximum of χ_L , while the line is the solution of the Eq.(21), with $h_c = 0.17$ and $T_{\text{CEP}} = 0.261$ GeV

$$\ln \det[\hat{Q}_F(\kappa)] \simeq (2N_f)(2N_c)(2\kappa)^{N_\tau} N_s^3 L_L. \quad (22)$$

A comparison of this equation in the mean-field approximation with the corresponding expression in the continuum model

$$\ln \det[\hat{Q}_F] \simeq VT^3 h(\beta m, N_f) L_L, \quad (23)$$

using $VT^3 = (N_s/N_\tau)^3$, yields a relation between the symmetry breaking parameter h in the continuum and the hopping parameter κ on the lattice

$$h(\beta m, N_f) \simeq (2N_f)(2N_c)(2\kappa)^{N_\tau} N_\tau^3. \quad (24)$$

In particular, for $\mu = 0$, one finds

$$(2\kappa)^{N_\tau} N_\tau^3 = \frac{(\beta m)^2}{2\pi^2} K_2(\beta m). \quad (25)$$

The right hand side of Eq.(25) represents a quantity in the continuum. The continuum extrapolation of the left hand side of Eq.(25) is however complicated, owing to the renormalization of the Polyakov loop and the bare quark masses represented by κ , in Eq.(22). Nevertheless, Eq.(25) indicates that $(2\kappa)^{N_\tau} N_\tau^3$ is presumably better suited for the continuum extrapolation, than the frequently used $(2\kappa)^{N_\tau}$ combination. Indeed, the lattice calculation in Ref. [16], yields a very strong N_τ dependence of $(2\kappa)^{N_\tau}$, consistent with the N_τ^3 scaling implied by Eq.(25). Thus, Eq.(25) can be considered as an alternative prescription for relating the hopping parameter to the quark mass.

However, the connection of κ to the physical quark mass remains ambiguous. Various conversion formulae have been proposed to determine the value of m_{CEP} [12, 16], showing

that $1 < m_{\text{CEP}} < 1.5 \text{ GeV}$ for $N_f = 3$. The present model calculation is consistent with this mass range.

A less ambiguous extraction of the physical quark masses at the deconfinement CEP can be performed by computing the ratio of the pseudoscalar to vector meson masses, $m_{\text{PS}}/m_{\text{V}}$. This ratio is expected to be close to unity if the heavy quark assumption is valid. An estimate of the critical quark mass m_{CEP} on the lattice can then be inferred from the heavy quarkonium spectrum. This, in conjunction with the matching formula (25), provides a consistency check for the continuum extraction of the critical strength of the symmetry breaking term.

IV. CONCLUSIONS

The dependence of the SU(3) deconfinement transition in the presence of heavy dynamical quarks on the number of flavors and on the quark mass was studied within an effective theory. We have formulated the thermodynamic potential of interacting heavy quarks and gluons in a mean-field approach, which reproduces the equation of state and the fluctuations of the Polyakov loop in SU(3) pure gauge theory.

We have explored the phase diagram at finite temperature and density for different quark masses and number of flavors. In order to examine the deconfinement critical endpoint (CEP) and its characteristics, we have studied fluctuations of the Polyakov loop.

It was shown, that the CEP can be uniquely identified by a singularity of the longitudinal Polyakov loop susceptibility. The transverse susceptibility, on the other hand, remains finite at the CEP, and is much smaller than at the first-order deconfinement transition.

At vanishing chemical potential, the critical endpoint ap-

pears at the quark mass, $m_{\text{CEP}} = 1.10, 1.35, 1.48 \text{ GeV}$, for $N_f = 1, 2$ and 3 flavors, respectively. The corresponding critical temperature, $T_{\text{CEP}} = 0.261 \text{ GeV}$ is 9 MeV below the deconfinement temperature in the pure SU(3) gauge theory.

The critical mass, m_{CEP} , was shown to be increasing with μ , whereas the critical temperature at the CEP is almost constant. Consequently, at finite density, the region of the first-order deconfinement phase transition shrinks with increasing μ .

We have discussed the relation between the model and lattice results. In particular, we have argued, that in order to obtain the continuum limit for the strength of the $Z(3)$ symmetry breaking term in the hopping parameter (κ) expansion, one should consider the product, $(2\kappa)^{N_\tau} N_\tau^3$, where N_τ is the lattice size in the temporal direction.

Finally, based on the matching criteria of the model and the lattice fermionic determinant, a formula connecting the hopping parameter and the quark mass was proposed.

V. ACKNOWLEDGMENTS

We acknowledge the stimulating discussions with Chihiro Sasaki, the BNL-Bielefeld lattice group, and the WHOT-QCD lattice Collaboration. P.M.L. is grateful for the helpful comments from Constantia Alexandrou. K. R. acknowledges fruitful discussions with Frithjof Karsch and Rob Pisarski. P.M.L. is supported by the Frankfurt Institute for Advanced Studies (FIAS). B. F. is supported in part by the Extreme Matter Institute EMMI. K. R. acknowledges partial support of the Polish National Science Center (NCN), under Maestro grant 2013/10/A/ST2/00106. The numerical calculations have been performed on the GridEngine Cluster at GSI.

-
- [1] J. Greensite, *Prog. Part. Nucl. Phys.* **51**, 1 (2003).
 - [2] G. 't Hooft, *Nucl. Phys. B* **138**, 1 (1978).
 - [3] L. G. Yaffe and B. Svetitsky, *Phys. Rev. D* **26**, 963 (1982).
 - [4] L. D. McLerran and B. Svetitsky, *Phys. Lett. B* **98**, 195 (1981); *Phys. Rev. D* **24**, 450 (1981).
 - [5] A. M. Polyakov, *Phys. Lett. B* **72**, 477 (1978).
 - [6] K. Binder, *Rep. Prog. Phys.* **50**, 783 (1987).
 - [7] F. Green and F. Karsch, *Nucl. Phys. B* **238**, 297 (1984).
 - [8] P. M. Lo, B. Friman, O. Kaczmarek, K. Redlich, and C. Sasaki, *Phys. Rev. D* **88**, 014506 (2013).
 - [9] C. McNeile, A. Bazavov, C. T. H. Davies, R. J. Dowdall, K. Hornbostel, G. P. Lepage and H. D. Trottier, *Phys. Rev. D* **87**, 034503 (2013).
 - [10] P. M. Lo, B. Friman, O. Kaczmarek, K. Redlich, and C. Sasaki, *Phys. Rev. D* **88**, 074502 (2013).
 - [11] F. Karsch, E. Laermann, and A. Peikert, *Nucl. Phys. B* **605**, 579 (2001).
 - [12] T. A. DeGrand and C. E. DeTar, *Nucl. Phys. B* **225**, 590 (1983).
 - [13] N. Attig, B. Petersson, M. Wolff, R. V. Gavai *Z. Phys. C - Particles and Fields* **40**, 471 (1988).
 - [14] J. Langelage and O. Philipsen, *JHEP* **1001**, 089 (2010).
 - [15] S. Ejiri *et al.* [WHOT-QCD Collaboration], *PoS LATTICE* **2012**, 089 (2012).
 - [16] C. Alexandrou, A. Borici, A. Feo, P. de Forcrand, A. Galli, F. Jergerlehner and T. Takaishi, *Phys. Rev. D* **60**, 034504 (1999).
 - [17] G. Aarts, O. Kaczmarek, F. Karsch and I. -O. Stamatescu, *Nucl. Phys. Proc. Suppl.* **106**, 456 (2002).
 - [18] M. Fromm, J. Langelage, S. Lottini, O. Philipsen *JHEP* **01**, 042 (2012).
 - [19] H. Saito, S. Ejiri, S. Aoki, T. Hatsuda, K. Kanaya, Y. Maezawa, H. Ohno, and T. Umeda, *Phys. Rev. D* **84**, 054502 (2011).
 - [20] K. Kashiwa, R. D. Pisarski and V. V. Skokov, *Phys. Rev. D* **85**, 114029 (2012).
 - [21] P. N. Meisinger, T. R. Miller, and M. C. Ogilvie, *Phys. Rev. D* **65**, 034009 (2002). P. N. Meisinger and M. C. Ogilvie, *Phys. Rev. D* **65**, 056013 (2002). P. N. Meisinger, M. C. Ogilvie and T. R. Miller, *Phys. Lett. B* **585** (2004) 149.
 - [22] D. J. Gross, R. D. Pisarski and L. G. Yaffe, *Rev. Mod. Phys.* **53** (1981) 43.
 - [23] H. T. Elze, D. E. Miller and K. Redlich, *Phys. Rev. D* **35**, 748 (1987).
 - [24] Y. Hatta and K. Fukushima, *Phys. Rev. D* **69**, 097502 (2004).
 - [25] C. Sasaki, B. Friman, and K. Redlich, *Phys. Rev. D* **75**, 074013

- (2007) .
- [26] C. Ratti, M. A. Thaler, and W. Weise, Phys. Rev. D **73**, 014019 (2006).
- [27] A. Dumitru, R. D. Pisarski and D. Zschiesche, Phys. Rev. D **72**, 065008 (2005) .